Volume 234, number 2, 367–373 FEB 06085 July 1988

The refined 2.3 Å crystal structure of human leukocyte elastase in a complex with a valine chloromethyl ketone inhibitor

Wei An-Zhi, Irmgard Mayr and Wolfram Bode

Max-Planck-Institut für Biochemie, D 8033 Martinsried, FRG

Received 16 May 1988

The stoichiometric complex formed between human leukocyte elastase and a synthetic MeO-Suc-Ala-Ala-Pro-Val chloromethyl ketone inhibitor was co-crystallized and its X-ray structure determined, using Patterson search methods. Its structure has been crystallographically refined to a final R value of 0.145 (8.0 and 2.3 Å). The enzyme structure is very similar to that recently observed in a complex formed with the ovomucoid third domain from turkey [(1986) EMBO J. 5,2453–2458]. The rms deviation of all α-carbon atoms is 0.32 Å. The peptidic inhibitor is bound in a similar overall conformation as the ovomucoid binding segment. Covalent bonds are formed between Val-P1 of the inhibitor and His-57 NE2 and Ser-195 OG of the enzyme. The carbonyl carbon is tetrahedrally deformed to a hemiketal. The valine side chain is arranged in the S1 pocket in the g^- conformation.

Elastase; Polypeptide inhibitor; Crystal structure; Serine proteinase; (Human leukocyte)

1. INTRODUCTION

Human leukocyte elastase (EC 3.4.21.37) is a lysosomal proteinase capable of degrading many connective tissue proteins such as elastin and destroying invading bacteria. Excessive leakage of this enzyme and reduced levels of functional natural inhibitors result in severe tissue damage, as observed for example in pulmonary emphysema, cystic fibrosis and adult respiratory distress syndrome [1,2]. Its importance as a pathogenic agent in various diseases has stimulated the search for protein inhibitors and synthetic inhibitors [3,4].

In order to understand the specificity of HLE and to rationalize the design of potent, selective inhibitors we have recently determined the X-ray crystal structure of HLE in its molecular complex with an ovomucoid inhibitor third domain from turkey (OMTKY3) [5]. Together with sequencing methods also the peptide sequence of HLE was established [5,6]. The HLE turned out to be a characteristic trypsin-like serine proteinase, with several surface segments possessing, however, a quite unique conformation.

The subsite specificity of HLE has been explored using peptidyl substrates and inhibitors with varying peptidic moieties [7–10]. In agreement with modeling results derived from its spatial structure [5] HLE exhibits a clear preference for P1 residues with medium-sized alkyl side chains such as valine. Specificity effects on binding and reactivity have been demonstrated up to the P6 position [11]. Excellent correlation was observed between peptide nitroanilide hydrolysis, peptide bond cleavage and chloromethyl ketone inhibition [7]. The most effective chloromethyl ketone inhibitor for HLE found thus far is MeO-Suc-Ala-Ala-Pro-Val chloromethyl ketone (MPCMK), which was shown to provide protection against induced emphysema in rat [1].

Correspondence address: W. Bode, Max-Planck-Institute für Biochemie, D 8033 Martinsried, FRG

Abbreviations: HLE, human leukocyte elastase; OMTKY3, ovomucoid third domain from turkey; MPCMK, methoxy succinyl-Ala-Ala-Pro-Val chloromethyl ketone; MPM, methoxy succinyl-Ala-Ala-Pro-Val methylene; HLE-MPM, covalent complex formed between MPCMK and HLE; MeO-Suc, methoxy succinyl; Vam, C-(methylene) valyl

Published by Elsevier Science Publishers B.V. (Biomedical Division)
00145793/88/$3.50

Chloromethyl ketones with distinct peptidyl moieties are potent, specifically reacting inhibitors of serine proteinases forming stable covalent complexes which are well suited for crystallographic studies [11–14]. We have co-crystallized the complex formed between MPCMK and HLE and determined its molecular structure. In the following we report its refined structure, with particular emphasis on the interactions of the MeO-Suc group and of the P1-valyl residue with the enzyme.

2. MATERIALS AND METHODS

Human leukocyte elastase (EC 3.4.21.37) was kindly denated by Drs S. Neumann and H. Lang of Merck AG (Darmstadt, FRG). MeO-Suc-Ala-Ala-Pro-ValCH_2Cl (MPCMK) was kindly provided by Dr J. Powers of the Georgia Institute of Technology (Atlanta, USA). All chemicals were purchased from Merck (Darmstadt).

HLE (9 mg/ml) was inhibited by a 10-fold molar excess of MPCMK at pH 6.5 for 30 min at 20°C. Unbound inhibitor was removed by dialysis. The stoichiometric complex was crystallized at 20°C in 1.2 M to 1.7 M ammonium sulphate, buffered with 0.1 M Tris-HCl to pH 9 and 8, respectively, using the hanging drop vapour diffusion technique. Short, almost isometric crystals of hexagonal shape, rounded edges and diameters up to 0.15 mm were obtained. According to Laue's symmetry and systematic extinctions these crystals are of hexagonal space group $P6_3$. The cell constants are $a = b = 74.2$ Å, $c = 70.6$ Å, $\alpha = \beta = 90°$, $\gamma = 120°$. These crystals contain one complex per asymmetric unit and show reflections to almost 2.0 Å resolution.

X-ray intensity data were collected on rotation/precession cameras using graphite monochromatized CuK_α radiation. From 3 native crystals soaked in 2.5 M ammonium sulphate at pH 8, 20 260 reflections to 2.3 Å were evaluated, using the FILME program as modified by W.S. Bennett, jr. These data were merged and scaled by means of the PROTEIN program package [15] yielding 7390 unique reflections which represent 75% of all data expected at a 2.3 Å resolution (with 35% completeness in the most outer shell from 2.4 to 2.3 Å). The final R merge (defined as $\Sigma|I - \langle I\rangle|/\Sigma|I|$) is 0.081.

The orientation of the HLE component in the crystals was determined by the rotation function in Patterson space using a model Patterson map (2400 highest peaks, 3–15 Å shell) calculated with the HLE component of the final HLE-OMTKY3 complex (R value of 0.162 with 1.8 Å data [16]) and the crystal Patterson map (calculated with intensity data from 8 to 3.5 Å). The positioning of the HLE molecule in the unit cell was achieved by a translation function search using programs written by E.E. Lattmann and intensity data from 8 to 3.5 Å. A similar result was obtained with a correlation coefficient searching program of S.J. Remington. The rotational and translational parameters were further refined with the Fourier transform fitting program TRAREF [17]. The crystallographic R value (defined as $\Sigma(||F_o| - |F_c||)/\Sigma|F_o|$) of the HLE model placed and oriented according to the resulting parameters was 0.39 for 8 to 3.5 Å data.

A 3 Å $2F_o - F_c$ Fourier map calculated with Sim-weighted model phases displayed clear electron density for the MPM inhibitor in addition to most of the HLE component. This inhibitor was constructed by linking a MeO-Suc group (MSU14I) to an Ala-15I–Ala-16I–Pro-17I–Val-18I peptide, whose valyl residue had been converted into a valyl methylene with tetrahedral geometry at the carbonyl carbon (Vam-18I) [13,18]. This inhibitor structure was modeled into the electron density on a PS330 interactive display (Evans and Sutherland) using the PSFRODO version [19] of FRODO [20]. The enzyme-inhibitor model was refined within 7 macrocycles using the energy restraint crystallographic refinement EREF [21] and energy parameters mentioned recently [22]; all nonbonded restraint parameters for Ser-195 OG and for the Vam-18I methylene were set to zero to allow their unbiased approach to Vam-18I carbonyl and His-57 NE2. Fourier and difference Fourier maps were repetitively inspected at the graphics display to correct gross model errors.

The intensity data used were gradually extended to a resolution of 2.3 Å. Solvent molecules were inserted at stereochemically reasonable positions if the difference electron density exceeded 2σ. Finally, also individual B values were refined and averaged for all main chain and side chain atoms of each residue separately. The final model parameters are given in table 1. The final R value for 7103 reflections of between 8 and 2.3 Å resolution is 0.145.

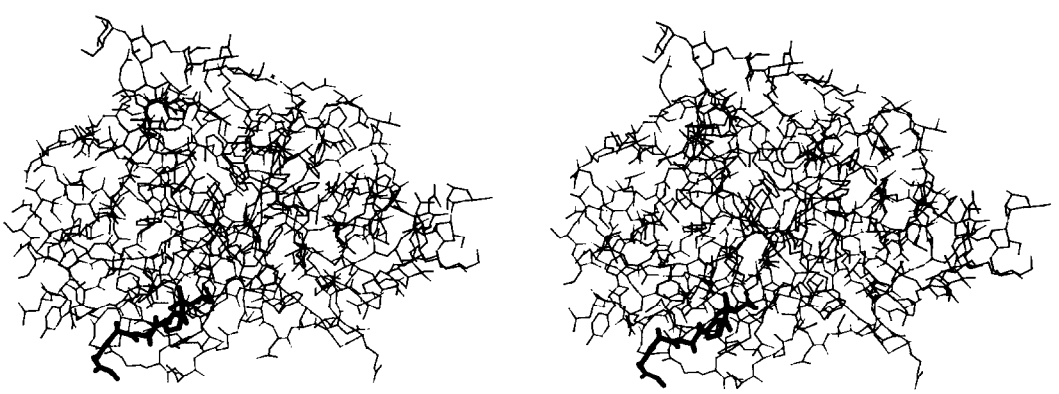

Fig.1. Complete model of the complex (leaving out all solvent molecules) of HLE (thin connections) and the MPM inhibitor (thick connections).

3. RESULTS

After extensive refinement the polypeptide chain of HLE can be traced from the amino-terminal residue Ile-16 to Arg-36, from Gly-39 to Gly-145 and from Arg-148 to Gln-243. Because HLE is present as a single chain (as shown by SDS-PAGE), the missing intermediate residues, Gly-38 and segment Arg-146–Asn-147 (which are defined in HLE-OMTKY3 [5]), are strongly disordered in the crystal structure. The last visible residue, Gln-243, is relatively poorly defined by electron density. According to carboxy-terminal sequencing data for medullasin [23] there might be a consecutive arginine residue at the carboxy-terminus, which is completely disordered. Except for this Arg-244 (see table 2) the electron density map is in agreement with the published amino acid sequence [6,23].

Table 1

Final model parameters of the HLE-MPM structure

Number of active protein atoms	1686
Number of active solvent atoms	162
rms standard deviation from target values	
Bond lengths	0.022 Å
Bond angles	2.79°
Total internal energy	−1186 kcal/mol
Resolution range	8–2.3 Å
Number of unique reflections used for refinement	7104
R value	0.145
Mean *B* value	13 Å^2
B value limits	5.0–60.0 Å^2
Estimated mean coordinate error from agreement between observed and calculated structure factor	
According to Luzzati [32]	0.20 Å
According to Cruickshank [33]	0.13 Å

Fig.1 shows the structure of the HLE-MPM complex in an orientation similar to that given for HLE-OMTKY3 [5]. The conformation of the HLE component is only very weakly affected by the different bound inhibitors and by the quite different cell contacts; the rms deviation of all α-carbon atoms is 0.32 Å, i.e. only slightly above the estimated coordinate errors (table 1). A few significant deviations are found at some exposed surface loops. A few sites, especially the side chains of Val-63A and Leu-223, and the loop 70–80 (comprising the 'Ca-loop' in trypsin [24]) are better

Table 2

Sequence numbering of HLE due to topological similarity with chymotrypsinogen

I16	V17	G18	G19	R20	R21	A22	R23	P24	H25
A26	W27	P28	F29	M30	V31	S32	L33	Q34	L35
R36	G38	G39	H40	F41	C42	G43	A44	T45	L46
I47	A48	P49	N50	F51	V52	M53	S54	A55	A56
H57*	C58	V59	A60	N61	V62	N63	V63A	R63B	A63C
V64	R65	V66	V67	L68	G69	A70	H71	N72	L73
S74	R75	R76	E77	P78	T79	R80	Q81	V82	F83
A84	V85	Q86	R87	I88	F89	E90	N92	G93	Y94
D95	P96	V97	N98	L99	L100	N101	D102*	I103	V104
I105	L106	Q107	L108	N109$^+$	G110	S111	A112	T113	I114
N115	A116	N117	V118	Q119	V120	A121	Q122	L123	P124
A125	Q126	G127	R128	R129	L130	G131	N132	G133	V134
Q135	C136	L137	A138	M139	G140	W141	G142	L143	L144
G145	R146	N147	R148	G150	I151	A152	S153	V154	L155
Q156	E157	L158	N159$^+$	V160	T161	V162	V163	T164	S165
L166	C168	R177	R178	S179	N180	V181	C182	T183	L184
V185	R186	G186A	R186B	Q187	A188	G189	V190	C191	F192
G193	D194	S195	G196	S197	P198	L199	V200	C201	N202
G207	L208	I209	H210	G211	I212	A213	S214	F215	V216
R217	G218	G219	C220	A220A	S221	G222	L223	Y224	P225
D226	A227	F228	A229	P230	V213	A232	Q233	F234	V235
N236	W237	I238	D239	S240	I241	I242	Q243		

* active site residues; $^+$, sugar attachment sites

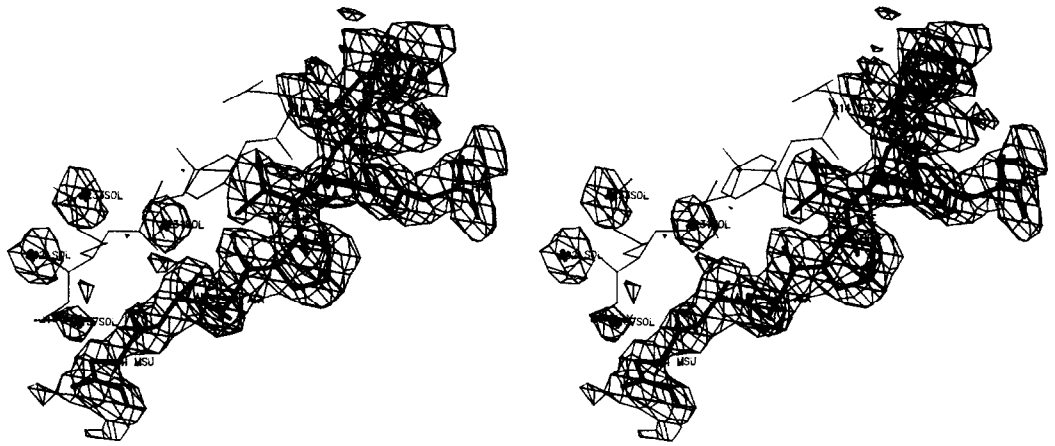

Fig.2. Section of the Fourier map around the MPM inhibitor. The map was calculated with phases derived from a model from which the complete inhibitor, the side chains of Ser-195 and His-57 and solvent molecules 702, 1137, 1231 and 1233 were omitted. Contour surface (restricted to these groups) is at 0.8σ.

defined in this structure than in the HLE-OMTKY3 complex, presumably due to stabilizing crystal contacts. All solvent molecules buried within the HLE components have equivalent counterparts in both HLE complexes.

Of the six related enzymes for which tertiary structures have been evaluated and deposited at the Brookhaven Protein Data Bank, HLE is topologically most equivalent [16] with porcine pancreatic elastase [25,26]. In table 2 HLE has been aligned relative to chymotrypsinogen on the basis of topological equivalences [16]. Similar to the HLE-OMTKY3 complex [5] and in agreement with findings upon peptide sequencing [6] two sugar chains (also shown in fig.1) are found, each *N*-asparagine-linked through *N*-acetyl-glucosamines; the Asn-109-linked carbohydrate is only defined for this linking sugar and an α-1,6-bound L-fucopyranose, whereas in the second carbohydrate, at Asn-159, two additional sugar rings (a β-1,4-linked *N*-acetyl-glucosamine and a branching mannose) are partially defined [16].

As shown in fig.2, the electron density map clearly shows the juxtaposition of the MPM inhibitor to the extended S4⟶S1 binding site of HLE. The density around the Vam-18I carbonyl is tetrahedrally shaped. Between the methylene carbon and the carbonyl carbon atoms of P1 residue Vam-18I and His-57 NE2 and Ser-195 OG of the enzyme, the densities defining inhibitor and enzyme groups merge indicating covalent bond formation and transition of the planar carbonyl group to a tetrahedral hemiketal (fig.3).

In contrast to the four amino acid residues 15I–18I, the MeO-Suc group is only poorly defined in the Fourier map. Experiments with alternative phasing models indicate that the MeO-Suc location shown in the figures is the most occupied. In this conformation it has, however, unfavourable contacts with atoms of symmetry related molecules, especially with the side chain of another Phe-192. The next probable alternative position of MeO-Suc marked by disconnected electron density lobes interpreted as solvent molecules 702, 1137, 1231 and 1233 (fig.2) is along the Arg-217 side chain, which is in a slightly different conformation compared with HLE-OMTKY3 (fig.4).

The four amino acid residues of the inhibitor are in relatively similar positions (the rms deviation of all common atoms is 0.44 Å) relative to the HLE binding site and in a similar conformation as the P4 to P1 residues of HLE-OMTKY3 (fig.4). Similar favourable intermolecular hydrogen bonds are formed between Ala-16I N and Val-216 O (2.8 Å) and Val-216 N and Ala-16I O (3.2 Å). Ala-16I is, together with Ala-15I, involved in several additional unspecific contacts with HLE residues Phe-215, Val-216 and Arg-217. Pro-17I (P2), like Thr-17I of OMTKY3 (fig.4), is embedded in the very characteristic hydrophobic S2 pocket of HLE, lined by the side chains of His-57

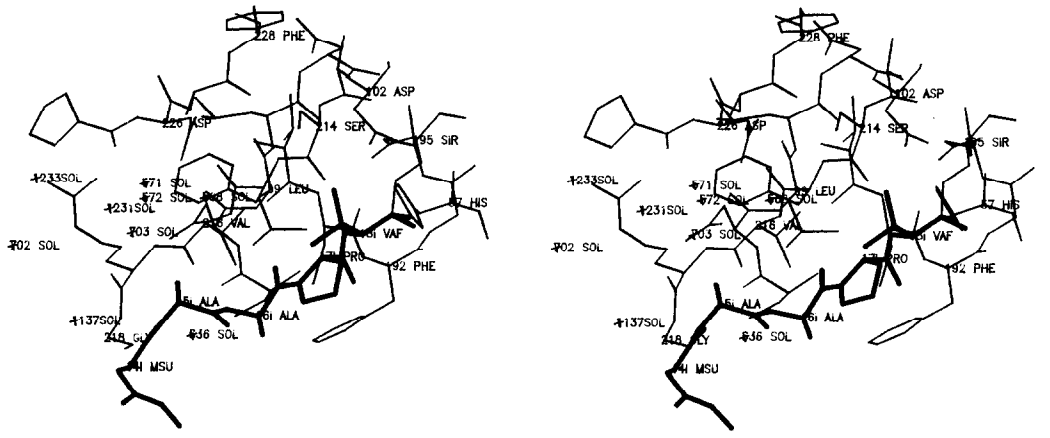

Fig.3. Section of the HLE-MPM structure around the bound inhibitor, with the inhibitor emphasized by thick lines.

(facing it with its flat side), Leu-99, Phe-192 and Phe-215 (fig.3).

The most significant deviations between both bound inhibitors are observed at their P1 residues, i.e. Leu-18I (OMTKY3) and Vam-18I. Vam-18I is tilted leaving the CA position almost unchanged, but enabling the amido nitrogen to approach Ser-214 O (to form an almost ideal hydrogen bond of 2.8 Å length), and the bulky Vam side chain to avoid unfavourable contacts with the S1 pocket of HLE. Vam CB is displaced 1.0 Å. The valyl side chain is arranged in the g^- conformation ($\chi 1 = -57°$). As a consequence of the shorter side chain of Vam-18I, compared with Leu-18I, the side chains of Val-190 and Val-216 (which are lining the pocket and are also g^- rotamers) turn slightly into the S1 pocket (with displacements of 0.9 Å at 216 CG1 and of 0.7 Å at 190 CG2), and 191 O moves towards Vam-18I CB, to shrink the incompletely refilled pocket.

This tilting of Vam-18I furthermore allows its carbonyl carbon to move 1.2 Å towards Ser-195 OG, which in turn must only slightly rotate (0.6 Å) to form a covalent bond under formation of a tetrahedral hemiketal group. That these displacements are not the result of the simultaneous formation of the covalent bond 18Imethylene-57NE2 is demonstrated by the similar structures of enzyme-aldehyde complexes [27] which lack this latter bond. The carbonyl group of Vam-18I is oriented

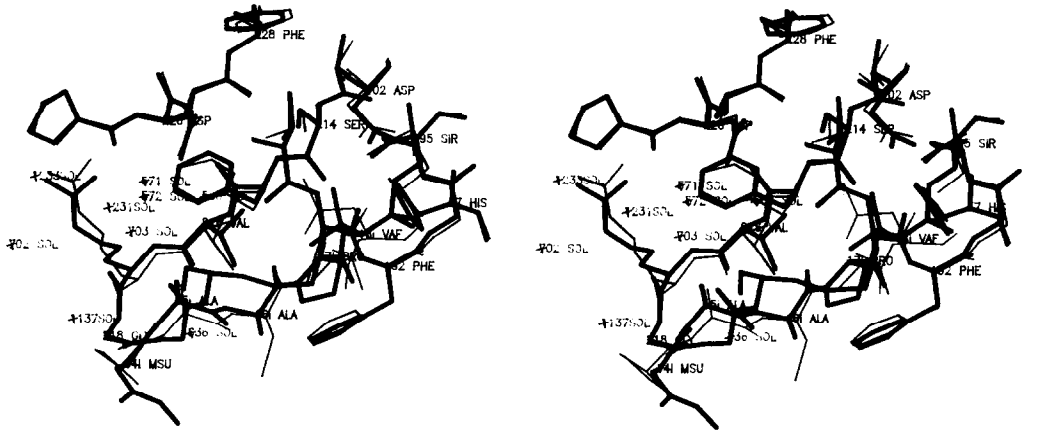

Fig.4. Section of the HLE-MPM structure around the MPM inhibitor (thick connections), overlayed with the identical or homologous residues of the HLE-OMTKY3 complex [5,16].

differently, with its oxygen, however, only slightly displaced 0.4 Å out of the oxyanion hole. Obviously (fig.4) the HLE main chain around Gly-193 follows this movement and still allows the formation of a 2.7 Å hydrogen bond from its amide nitrogen to Vam-18I O (besides the other 3.3 Å bond from Ser-195 N).

4. DISCUSSION

The rational design of potent synthetic peptidic inhibitors of HLE requires a detailed understanding of the HLE binding site and of its interaction with the peptidyl moiety, as is currently only achieved by X-ray crystallography. To date we have been able to obtain, besides several HLE complexes with protein inhibitors like OMTKY3 [16], only crystals of free or PMSF substituted HLE of bad diffraction quality and thus unsuitable for soaking experiments with small synthetic inhibitors. This work represents the first example of the creation of HLE complex crystals by co-crystallization, to get a detailed picture of the interaction site.

In general, the overall arrangement of the MPM inhibitor is similar to that one would expect from knowledge of the OMTKY3 binding segment, and the formation of two covalent bonds to enzyme reactive site groups are as observed in related enzyme-peptide inhibitor complexes [11–14]: the P1 residue of the inhibitor is pulled into the S1 pocket, with the strengthening of the hydrogen bond between its amido nitrogen and Ser-214 O, and with simultaneous pyramidalisation of its carbonyl function and addition of Ser-195 OG. The structural state observed is similar to the presumed transition state of substrates during catalytic cleavage, and the movements and deformations mentioned are anticipated to be necessary to attain and to pass this transition state.

Two sites of this inhibitor are of particular interest:

(i) Binding to and modification of arginine residues [28] leads to inactivation of HLE, and Arg-217 localized closest to its reactive site residues and somewhat representing the S5 subsite [5] is most probably the cause of this inactivation. The MeO-Suc group (P5) could have been placed close to Arg-217, but seems to prefer another position. Nevertheless, a related P5 residue with an acidic end group could prefer to interact with the guanidyl group of Arg-217, which in turn could be pulled out of the closed enzyme protein surface, thus giving rise to inactivating conformational changes at the reactive site (through Asp-226?).

(ii) The comparison of the P1 residue Vam-18I with Leu-18I in HEL-OMTKY3 demonstrates that the valine residue is (possibly also through covalent interactions with Ser-195 OG) slightly tilted at its main chain, thus avoiding unfavourable contacts of its bulky side chain which would occur if its CA-CB dihedral were identical to that in Leu-18I. The slightly smaller space required by the valyl side chain is accommodated by the enzyme by small rotations of surrounding groups which lead to a slight reduction of the empty space available in the S1 pocket [16]. Nevertheless, the pocket is not fully occupied; due to its hydrophobic nature [5], a solvent molecule is, however, not accepted. The side chain conformation of Vam-18I is g^-, which makes it a less frequently observed but still favourable rotamer [29]. An isoleucine at P1 in an equivalent K1 conformation, with its CD atom in *trans*-position to CA (g^--*t* rotamer), could fill the pocket better, thus explaining its slightly higher preference in substrates for HLE compared with valine [9].

Several potent protein inhibitors of HLE, especially those engineered to attain improved binding and stability properties, have a valine at P1. In ovomucoid inhibitors, valine at P1 slightly reduces the binding properties compared with leucine [30], whereas semi-synthetically modified BPTI-based inhibitors gain in affinity by a Leu⟶Val replacement [31]. This work giving the probable conformation of a bound Val-P1 residue provides an initial basis to model these structures.

NOTE ADDED IN PROOF

Unfortunately, we have overlooked two recent papers which report on the mechanism of HLE inactivation by this valine chloromethyl ketone [34] and on similar crystals of HLE complex with alanine chloromethyl ketone [35].

Acknowledgements: We thank M. Schneider and Dr R. Huber for computational assistance. This work has been supported by the Sonderforschungsbereich 207 of the Deutsche Forschungsgemeinschaft (grant H-1).

REFERENCES

[1] Powers, J.C. (1983) Am. Rev. Resp. Dis. 127, S54–S58.
[2] Janoff, A. (1985) Annu. Rev. Med. 36, 207–216.
[3] Stein, R.L., Trainor, D.A. and Wildonger, R.A. (1985) Annu. Rep. Med. Chem. 20, 237–246.
[4] Trainor, D.A. (1987) Trends Pharmacol. Sci. 8, 303–307.
[5] Bode, W., Wei, A.Z., Huber, R., Meyer, E., Travis, J. and Neumann, S. (1986) EMBO J. 5, 2453–2458.
[6] Sinha, S., Watorek, W., Karr, S., Giles, J., Bode, W. and Travis, J. (1987) Proc. Natl. Acad. Sci. USA 84, 2228–2232.
[7] Powers, J.C., Gupton, B.F., Harley, A.D., Nishino, N. and Whitley, R.J. (1977) Biochim. Biophys. Acta 485, 156–166.
[8] Nakajima, K., Powers, J.C., Ashe, B. and Zimmerman, M. (1979) J. Biol. Chem. 254, 4027–4032.
[9] McRae, B., Nakajima, K., Travis, J. and Powers, J.C. (1980) Biochemistry 19, 3973–3978.
[10] Lentini, A., Farchione, F., Ternai, B., Kreua-Ongarjnukod, N. and Tovivich, P. (1987) Biol. Chem. Hoppe-Seyler 368, 369–378.
[11] Lestienne, P. and Bieth, J.G. (1980) J. Biol. Chem. 255, 9289–9294.
[12] Poulos, T.L., Alden, R.A., Freer, S.T., Birktoft, J.J. and Kraut, J. (1976) J. Biol. Chem. 252, 1097–1103.
[13] Scott, A.I., Mackenzie, N.E., Malthouse, J.P.G., Primrose, W.V., Fagerness, P.E., Boisson, A., Li, Z.Q., Bode, W., Carter, C.M. and Jang, Y.J. (1986) Tetrahedron 42, 3269–3276.
[14] Betzel, C., Pal, G.P., Struck, M., Jany, K.-D. and Sänger, W. (1986) FEBS Lett. 197, 105–110.
[15] Steigemann, W. (1974) Dissertation, TU München.
[16] Bode, W. and Wei, A.Z., in preparation.
[17] Huber, R. and Schneider, M. (1985) J. Appl. Crystallogr. 18, 165–169.
[18] Walter, J. and Bode, W. (1983) Hoppe-Seyler's Z. Physiol. Chem. 364, 949–959.
[19] Pflugrath, J.W., Saper, M.A. and Quiocho, F.A. (1984) in: Methods and Application in Crystallographic Computing (Hall, S. and Ashiaka, T. eds) p.407, Clarendon Press, Oxford.
[20] Jones, T.A. (1978) J. Appl. Crystallogr. 11, 268–272.
[21] Jack, A. and Levitt, M. (1978) Acta Crystallogr. A34, 931–935.
[22] Bode, W., Papamokos, E. and Musil, D. (1987) Eur. J. Biochem. 166, 637.
[23] Okano, K., Aoki, Y., Sakurai, T., Kajitani, M., Kanai, S., Shimazu, T., Shimizu, H. and Naruto, M. (1987) J. Biochem. 102, 13–16.
[24] Bode, W. and Schwager, P. (1975) J. Mol. Biol. 98, 693–717.
[25] Sawyer, L., Shotton, D.M., Campbell, J.W., Wendell, P.L., Muirhead, H., Watson, H.C., Diamond, R. and Ladner, R.C. (1978) J. Mol. Biol. 118, 137–208.
[26] Meyer, E., Cole, G., Radakrishnan, R. and Epp, O. (1988) Acta Crystallogr. B44, 26–38.
[27] Walter, J., Radakrishnan, R., Meyer, E.F. and Bode, W., in preparation.
[28] Baici, A., Salgam, P., Fehr, K. and Böni, A. (1980) Biochem. Pharmacol. 29, 1723–1727.
[29] Janin, J., Wodak, S., Levitt, M. and Maigret, B. (1978) J. Mol. Biol. 235, 357–386.
[30] Laskowski, M., personal communication.
[31] Tschesche, H., Beckmann, J., Mehlich, A., Schnabel, E., Truscheit, E. and Wenzel, H. (1987) Biochim. Biophys. Acta 913, 97–101.
[32] Luzzati, V. (1952) Acta Crystallogr. 5, 802–810.
[33] Cruickshank, D.W.J. (1949) Acta Crystallogr. 2, 65–82.
[34] Stein, R. and Trainor, D.A. (1986) Biochemistry 25, 5414–5419.
[35] Williams, H.R., Lin. T.-Y., Navia, M.A., Springer, J.P., Keever, B.M., Hoogsteen, K. and Dorn, C.P. (1987) J. Biol. Chem. 262, 17178–17181.